Electronic Supplementary Material (ESI) for ChemComm.

Surface chemical state evaluation of $CoSe_2$ catalyst for oxygen evolution reaction

Chengzhe Zhang[a], Bo Tang[b], Xiaocong Gu[a] and Ligang Feng[a*]

a. School of Chemistry and Chemical Engineering, Yangzhou University, Yangzhou 225002, PR China.

b. School of Municipal and Environmental Engineering, Harbin Institute of Technology, Harbin 150090, China

Email: ligang.feng@yzu.edu.cn; fenglg11@gmail.com (L Feng*);

Experimental methods

Chemicals

All chemicals were analytical grade and used without further purification. Cobaltous nitrate hexahydrate [$Co(NO_3)_2 \cdot 6H_2O$], Selenium powder [Se], polyvinylpyrrolidone [PVP], ethylene glycol and potassium hydroxide [KOH] were obtained from Aladdin Bio-Chem Technology Co. LTD. (Shanghai, China). Nafion (5 wt%) and ethanol were purchased from Sigma-Aldrich. Deionized water was purified using a water purification system with the resistance of 18.2 MΩ (Thermo Fisher Scientific Co. LTD, USA).

Synthesis of $CoSe_2$

$CoSe_2$ catalysts were synthesized by a facile solvothermal method as following: 8 mg of Se powder and 58 mg of $Co(NO_3)_2 \cdot 6H_2O$ were firstly added into 65 mL of ethylene glycol with low magnetic stirring, and then 200 mg of PVP was dissolved in the solution with continuous stirring for 10 min. Afterwards, the mixture was transferred into a Teflon-lined stainless steel autoclave and maintained at 200 ^{o}C for 24 h. After the autoclave cooled down to room temperature, the black powder was washed with ethanol and deionized water for several times. Finally, the product was dried in a vacuum oven at 60 ^{o}C for overnight and denoted as $CoSe_2$-200. In addition, other $CoSe_2$ catalysts were synthesized with the controllable temperature of 180^{o}C and 220^{o}C, and numbered as $CoSe_2$-180 and $CoSe_2$-220.

Characterizations

The crystal structure of all $CoSe_2$ catalysts were conducted by Powder X-ray diffraction (XRD, Bruker D8 X-ray diffractometer) using a Cu Kα (λ = 1.5405 Å) radiation source operating at 40 kV and 40 mA at a scanning rate of 5° min^{-1}. The chemical composition of samples was examined by X-ray photoelectron spectroscopy (XPS, ECSALAB 250Xi, Al Kα radiation). The morphologies of all $CoSe_2$ catalysts were observed through the scanning electron microscopy (SEM, FEI Sirion-200). The crystalline structure of all $CoSe_2$ catalysts was analyzed by the transmission electron microscope (TEM, Philips, TECNAI 12, Holland). Energy-dispersive X-ray spectroscopy (EDX) image was obtained on a TECNAI G2 F30 transmission electron microscope (acceleration voltage:

300 kV).

Catalytic activity test

(1) Electrochemical measurements

All the electrochemical measurements, including cyclic voltammograms (CV), electrochemical impedance spectroscopy (EIS), electrochemical double-layer capacitances (C_{dl}), the linear sweep voltammograms (LSV) and chronoamperometry (CA) were carried out with a Bio-Logic VSP electrochemical workstation (Bio-Logic Co, France).

The conventional three-electrode system was applied and all potential are converted and referred to reversible hydrogen electrode (RHE), E (RHE) = E (SCE) + 0.0591 pH + 0.242 V. The $CoSe_2$ catalysts deposited glassy carbon electrode (d=3mm) acted as the working electrode, the graphite rod served as the counter electrode and the saturated calomel electrode (SCE) was used as the reference electrode via a double-salt bridge and luggin capillary tip close to the working electrode, and it was calibrated before and after use to make sure the accuracy. To prepare the working electrode, 2 mg of the $CoSe_2$ catalyst and 0.4 mg of carbon black were dispersed in 380 µL of ethanol with additional 20 µL of Nafion and the mixture was bath-sonicated for 30 min to form a well-dispersed ink. And then, 5 µL of the ink was dropped onto the polished glassy carbon electrode. Before the electrochemical measurements, the 1M KOH electrolyte was saturated with nitrogen for 30 min to remove the oxygen. For comparison, a commercial RuO_2 was also compared in the identical condition.

(2) CV and LSV

The CV curves and LSV curves of all $CoSe_2$ catalysts were measured in 1 M KOH solution with the applied potential from 1.045 V to 1.645 V vs. RHE and scan rate of 5 mV s^{-1}. IR compensation was all done by positive feedback of compensating 80% of the uncompensated solution resistance.

(3) Tafel analysis

The Tafel slope was calculated from the following equation: $\eta = a + b \log (j)$, where η is the overpotential (mV), b is the Tafel slope and j is the current density. The Tafel slope was calculated from 100% iR free LSV curves.

(4) ECSA measurements and calculations

The electrochemically active surface area (ECSA) of all $CoSe_2$ catalysts was obtained according to the equation: ECSA=R_f*S, where S is generally equal to the geometric area of the working electrode (In this work, S=0.07 cm^2) and R_f is the roughness factor. Meanwhile, the value of R_f is determined by the relation $R_f=(C_{dl}/0.07)/40$,[1] where the double-layer capacitance (C_{dl})is estimated by plotting the current (i) at various scan rates from 10 to 50 mV s^{-1}. The applied potential was 1.047-1.147 V vs. RHE in 1 M KOH solution.

(5) Electrochemical Impedance Measurements

Electrochemical impedance spectroscopy measurement was done with the frequency from 1000 kHz to 10 mHz with an amplitude of 5 mV at η=310 mV.

(6) Stability test and Chronoamperometry measurements

The dynamic stability was tested by cyclic voltammograms (CV) at the scan rate of 100 mV s^{-1} for 1000 cycles. After 1000 cycles, the polarization curve was compared with its initial curve. To further estimate the stability of the catalysts, the chronoamperometry (CA) was performed in 1 M KOH solution at a potential of 1.54 V vs. RHE for 15 h.

(7) Specific activity and Turnover of frequency (TOF) calculations

The specific activity is obtained by normalizing the apparent current to ECSA. The TOF (s^{-1}) can be calculated with the following equation TOF (s^{-1}) = I/(2*F*n), where I is the current (A) during linear sweep measurement, F is the Faraday's constant (96485.3 C/mol), n is the number of active sites (mol) (by assuming Co as the active sites). The factor 4 is based on the consideration that two electrons are required to produce one oxygen molecule.

Density functional calculations

Periodic DFT calculations were performed on the CASTEP code to investigate the oxygen evolution reaction on the catalyst surface. The exchange-correlation energy was treated with the PBE functional of generalize gradient approximation (GGA) form. The electronic wave functions at each k-point were expanded in terms of a plane-wave basis set, and an energy cutoff of 380 eV was employed. With the application of ultrasoft pseudopotential (USP), the sampling over the Brillouin zone (BZ) was treated by a (4×4×1) Monkhorst-Pack mesh. Moreover, several surfaces models are studied in this work: a slab of $CoSe_2$ which is extended in [210] direction, and the same slab which a surface Se atom is replaced with Co atom. The size of unit cells considered for the computations are ~ 13.00 Å × 11.50 Å × 20.00 Å. These models are large enough to accommodate the adsorbed species (e.g., O_2) while avoiding lateral interactions. The whole optimization procedure was repeated until the average force on the atoms was less than 0.01 eV $Å^{-1}$ and the energy change was less than 2.0×10^{-6} eV/atom. The stable configurations were obtained by geometry optimization from the ideal unrelaxed structures.

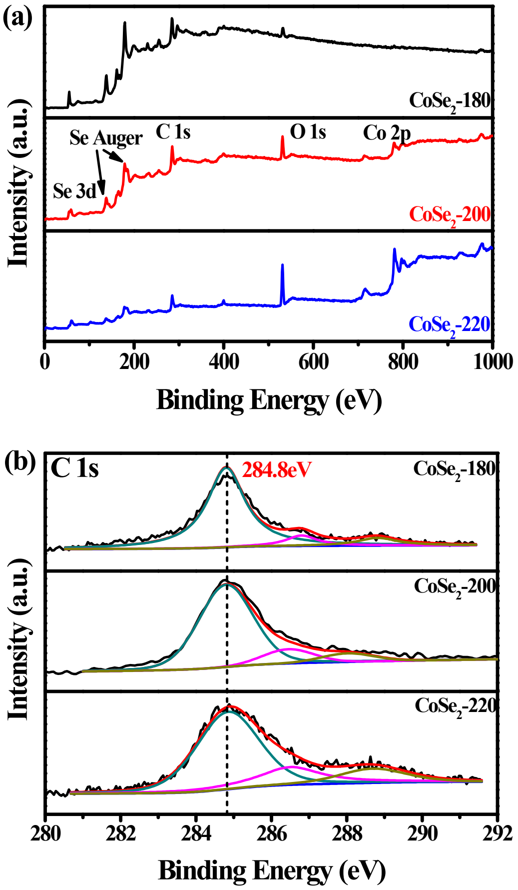

Figure S1. XPS survey spectrum of CoSe$_2$-180, CoSe$_2$-200, CoSe$_2$-220 (a) and High-resolution XPS spectra of C 1s (b).

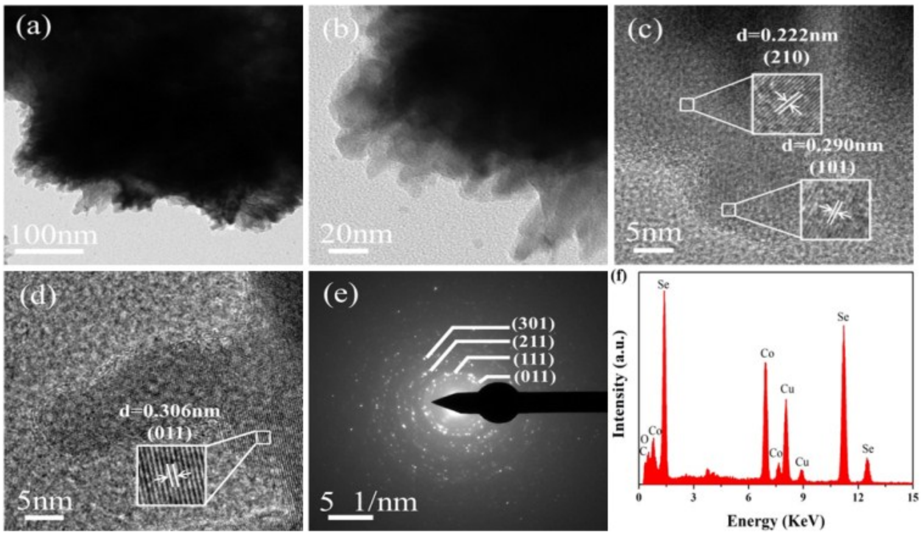

Figure S2. TEM (a,b), HRTEM (c-d), selected area electron diffraction pattern (e) and corresponding EDX spectrum (f) images of $CoSe_2$-200.

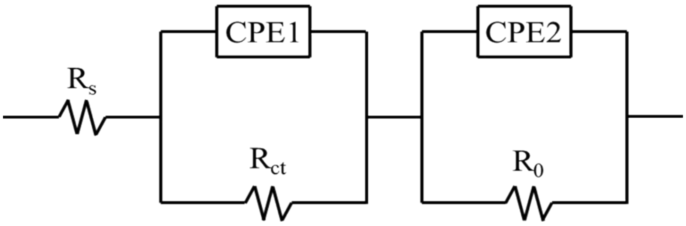

Figure S3. The equivalent circuit of the electrochemical process.

R_s is the solution resistance, R_{ct} and R_0 represent interfacial charge transfer resistance and adsorption resistance respectively. CPE1 and CPE2 are constant phase elements for the double layer capacitance.

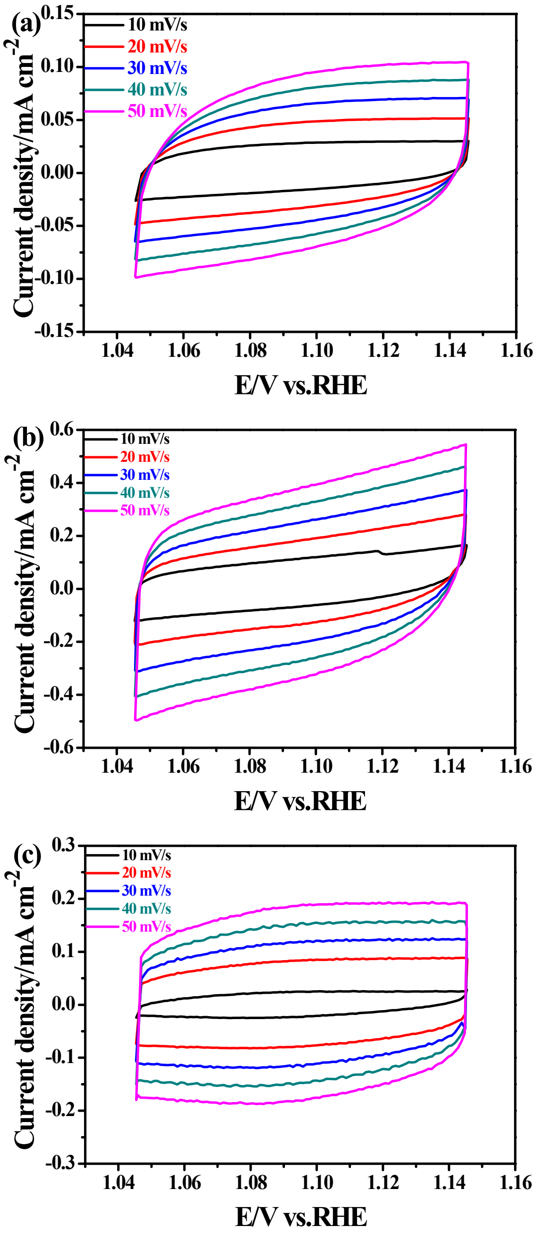

Figure S4. Cyclic voltammograms for the double layer capacitance from 1.047 to 1.147 V for $CoSe_2$-180 (a), $CoSe_2$-200 (b) and $CoSe_2$-220 (c) with various scan rates (10–50 mV/s), respectively.

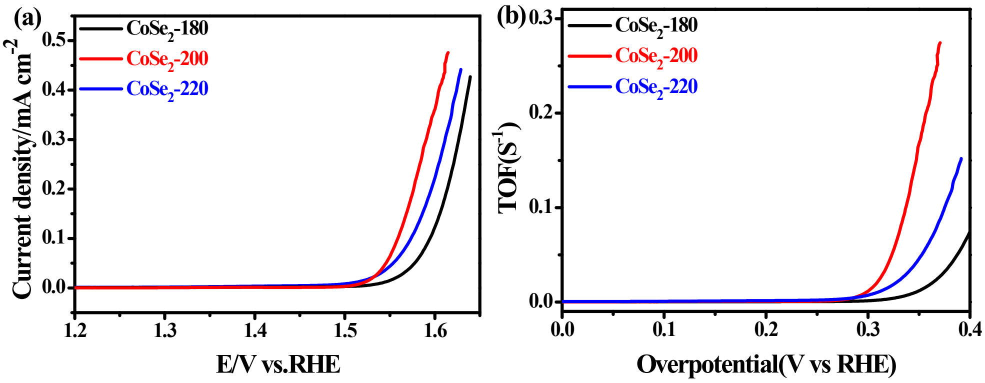

Figure S5. (a) Specific activity at the scan rate of 5 mV s^{-1} in 1 M KOH by normalizing the raw current to the electrochemical surface area and (b) TOF value of the $CoSe_2$-180, $CoSe_2$-200 and $CoSe_2$-220, respectively.

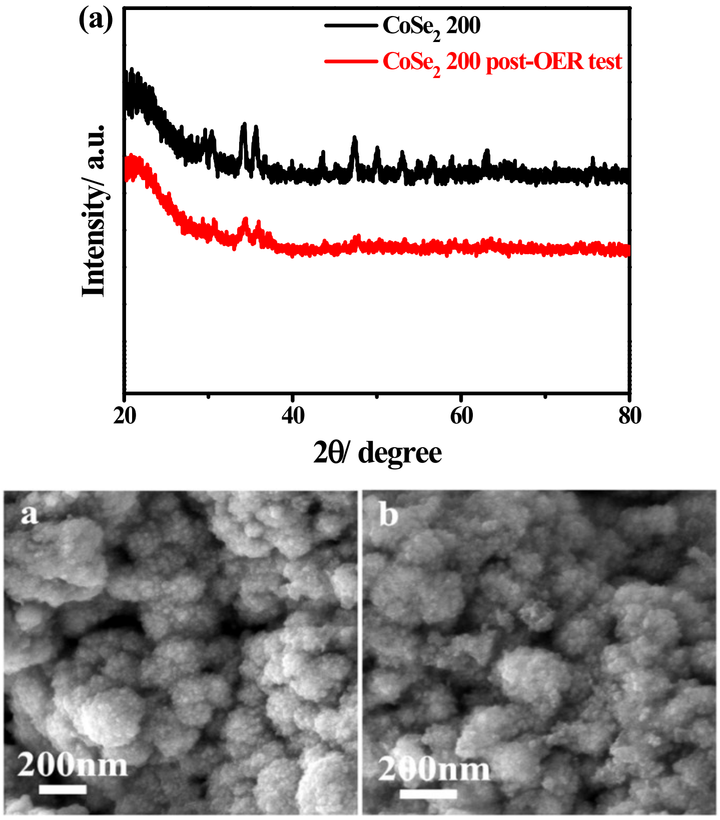

Figure S6a. XRD patterns of CoSe2-200 before and after OER test (Top) and SEM images of CoSe2-200 after OER Test (bottom).

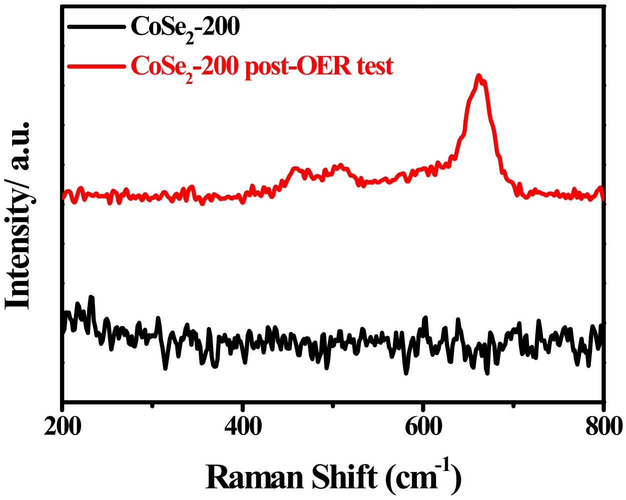

Figure S6b. Raman spectra of $CoSe_2$-200 and $CoSe_2$-200 after OER studies.

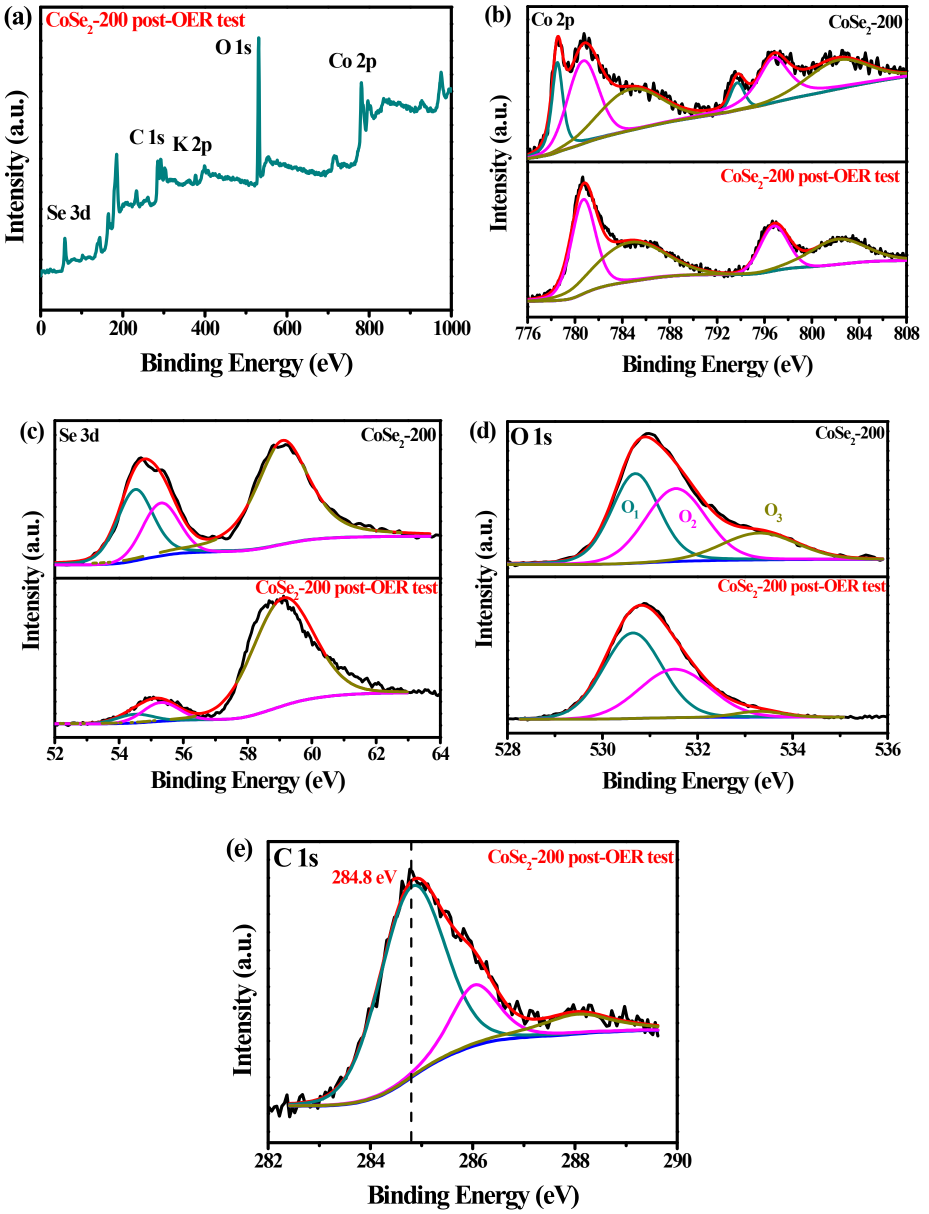

Figure S7. (a) Full-scan XPS spectrum of $CoSe_2$-200 after OER studies. High-resolution XPS spectra of Co 2p (b), Se 3d (c), O 1s (d) of $CoSe_2$-200 and $CoSe_2$-200 after OER studies. C 1s (e) XPS spectra for $CoSe_2$-200 after OER studies.

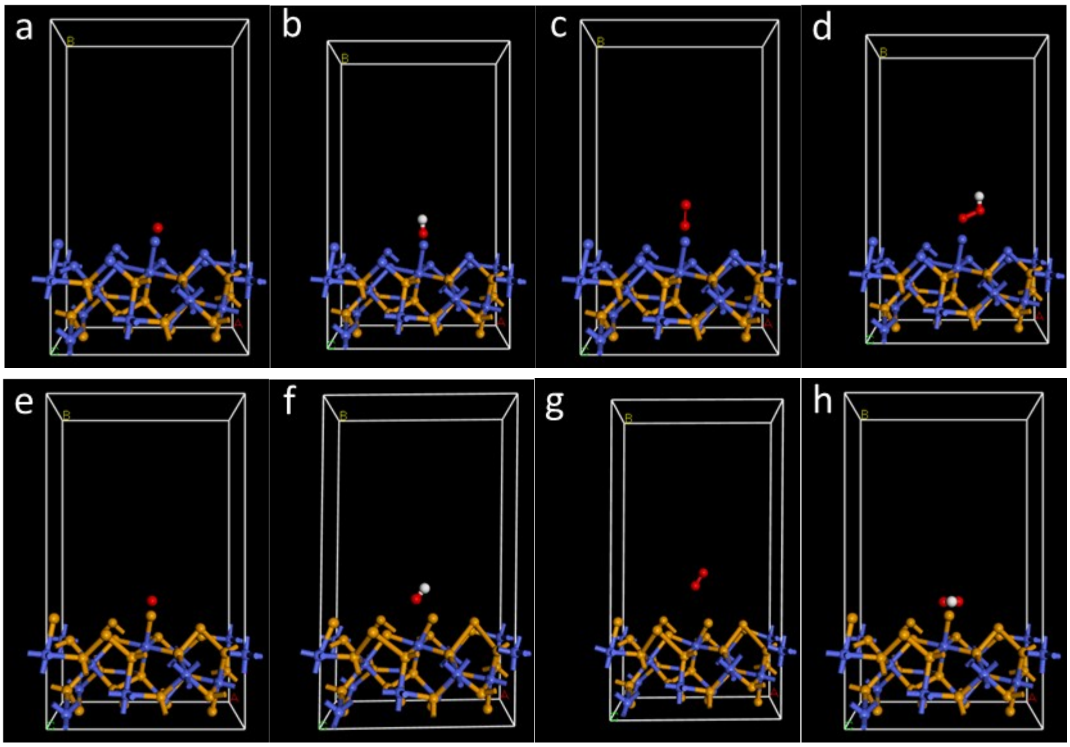

Figure S8. (a) Co-O, (b) Co-O, (c) Co-OO, (d) Co-OOH, (e) Se-O, (f) Se-OH, (g) Se-OO and (h) Se-OOH with the adsorption energy (AE) model for the DFT calculations.

Table S1. Surface composition for all $CoSe_2$ catalysts.

Samples	Contents (%)		
	Co	Se	O
$CoSe_2$-180	N/A	70.82	29.18
$CoSe_2$-200	7.30	25.55	67.15
$CoSe_2$-220	14.70	6.19	79.11

Note: Oxygen may also come from the contamination or adsorbed water/oxygen.

Table S2. The XPS peak position of Co $2p_{3/2}$ and Se 3d for all $CoSe_2$ catalysts.

Samples	Peak position (eV)			
	Co $2p_{3/2}$		Se 3d	
	Co-Se	Co-O	Se $3d_{5/2}$	Se$3d_{3/2}$
$CoSe_2$-180	778.6	780.8	54.8	55.7
$CoSe_2$-200	778.6	780.8	54.5	55.4
$CoSe_2$-220	778.6	780.8	54.5	55.4

Table S3. Quantitative XPS analysis of Co $2p_{3/2}$, Se 3d and SeO_x for all $CoSe_2$ catalysts.

Samples	Contents (%)			
	Co-Se	Co-O	Se 3d	SeO_x
$CoSe_2$-180	44	56	87(Se-Se)	13
$CoSe_2$-200	33	67	41(Se-Co)	59
$CoSe_2$-220	20	80	24(Se-Co)	76

Table S4. The XPS peak position of O 1s for all $CoSe_2$ catalysts.

Samples	Peak position (eV)		
	O_1(Co-O)	O_2(hydroxyl-)	O_3(physic/chemical adsorbed water)
$CoSe_2$-180	530.6	531.6	533.3
$CoSe_2$-200	530.6	531.6	533.3
$CoSe_2$-220	530.6	531.6	533.3

Table S5. Quantitative XPS analysis of O 1s for all $CoSe_2$ catalysts.

Samples	Peak position (eV)		
	O_1(Co-O)	O_2(hydroxyl-)	O_3(physic/chemical adsorbed water)
$CoSe_2$-180	17.6	44.8	37.6
$CoSe_2$-200	41.5	40.4	18.1
$CoSe_2$-220	57.2	39.9	2.9

Table S6. The comparison of some representative OER electrocatalysts in alkaline electrolyte.

Materials	Electrolyte	Overpotential (mV) @ 10 mA cm^{-2}	Tafel slope (mV dec^{-1})	Reference
$CoSe_2$-200	**1 M KOH**	**310**	**36**	**This work**
Prussian blue analogue-derived $CoSe_2$ nanoboxes	**1 M KOH**	**335**	**54.2**	[3]
MOF-derived $CoSe_2$ nanoparticles	**1 M KOH**	**330**	**79**	[4]
$CoSe_2$ nanocrystals	**1 M KOH**	**430**	**50**	[5]
Single-unit cell thick $CoSe_2$ nanosheets	**1 M KOH**	**350 (±1)**	**64**	[6]
$CoSe_2$ nanobelt	**0.1 M KOH**	**460**	**66**	[7]
Ultrathin $CoSe_2$ nanosheets	**0.1 M KOH**	**320**	**44**	[8]
ZIF-$Co_{0.85}Se$	**1M KOH**	**360**	**62**	[9]
1.0% Ag-$CoSe_2$ lamellar nanobelts	**0.1 M KOH**	**320**	**56**	[10]
$Au_{25}/CoSe_2$ nanosheets	**0.1 M KOH**	**430**	**80**	[11]
Zn-doped $CoSe_2$/CFC	**1 M KOH**	**356**	**88**	[12]
$Ni_{0.88}Co_{1.22}Se_4$ hollow microparticles	**1 M KOH**	**320**	**78**	[13]

Table S7. EIS fitting parameters from equivalent circuits for different catalyst samples.

Sample	R_s (Ω)	R_{ct} (Ω)	CPE1/S S^{-n}	R_0 (Ω)	CPE2/S S^{-n}
$CoSe_2$-180	8.21	100.1	1.43E-8	50.3	3.79E-4
$CoSe_2$-200	8.21	50.3	1.43E-8	10.0	3.79E-4
$CoSe_2$-220	8.32	545.7	8.95E-5	102.7	3.73E-5

Table S8. The XPS peak position of Co $2p_{3/2}$ and Se 3d for $CoSe_2$-200 and $CoSe_2$-200 after OER studies.

Samples	Peak position (eV)			
	Co $2p_{3/2}$		Se 3d	
	Co-Se	Co-O	Se $3d_{5/2}$	Se$3d_{3/2}$
$CoSe_2$-200	778.6	780.8	54.5	55.4
$CoSe_2$-200 after OER studies	778.6	780.8	54.5	55.4

Table S9. Quantitative XPS analysis of Co $2p_{3/2}$, Se 3d and SeO_x for $CoSe_2$-200 and $CoSe_2$-200 after OER studies.

Samples	Contents (%)			
	Co-Se	Co-O	Se 3d	SeO_x
$CoSe_2$-200	33	67	41	59
$CoSe_2$-200 after OER studies	1	99	12	88

Table S10. The XPS peak position of O 1s for $CoSe_2$-200 and $CoSe_2$-200 after OER studies.

Samples	Peak position (eV)		
	O_1(Co-O)	O_2(hydroxyl-)	O_3(physic/chemical adsorbed water)
$CoSe_2$-200	530.6	531.6	533.3
$CoSe_2$-200 post-OER test	530.6	531.6	533.3

Table S11. Quantitative XPS analysis of O 1s for $CoSe_2$-200 and $CoSe_2$-200 after OER studies.

Samples	Contents (%)		
	O_1(Co-O)	O_3(hydroxyl-)	O_4(physic/chemical adsorbed water)
$CoSe_2$-200	41.5	40.4	18.1
$CoSe_2$-200 after OER studies	58.4	38.5	3.1

Table S12. The models and adsorption energy (AE) of $CoSe_2$ with Co atom exposed ($CoSe_2$/Co) and $CoSe_2$ with Se atom exposed ($CoSe_2$/Se) for OER.

models	Adsorbed species	Adsorption energy (eV)	V (Å^3)	Height (Å)	Area (Å^2)	Adsorption energy per unit area (J/m^2)
$CoSe_2$/Co	-OH*	-4.152	1694.0	22.8	74.3	-0.90
	-O*	-7.560	1677.1	23.0	73.0	-1.66
	-OOH*	-3.491	1706.5	22.2	76.8	-0.73
	-O_2*	-1.750	1643.8	22.6	72.7	-0.39
$CoSe_2$/Se	-OH*	-3.277	1665.3	22.2	74.9	-0.70
	-O*	-4.907	1677.9	22.6	74.3	-1.06
	-OOH*	-8.105	1673.8	22.9	73.2	-1.77
	-O_2*	-0.595	1782.2	24.0	74.2	-0.13

References

1. C. C. L. McCrory, S. Jung, J. C. Peters and T. F. Jaramillo, *J. Am. Chem. Soc.*, 2013, **135**, 16977-16987.
2. C. Xia, Q. Jiang, C. Zhao, M. N. Hedhili and H. N. Alshareef, *Adv. Mater.*, 2016, **28**, 77-85.
3. V. Ganesan and J. Kim, *Mater. Lett.*, 2018, **223**, 49-52.
4. X. Liu, Y. Liu and L.-Z. Fan, *J. Mater. Chem. A*, 2017, **5**, 15310-15314.
5. I. H. Kwak, H. S. Im, D. M. Jang, Y. W. Kim, K. Park, Y. R. Lim, E. H. Cha and J. Park, *ACS Appl. Mater. Interfaces*, 2016, **8**, 5327-5334.
6. L. Liang, H. Cheng, F. Lei, J. Han, S. Gao, C. Wang, Y. Sun, S. Qamar, S. Wei and Y. Xie, *Angew. Chem., Int. Ed.* , 2015, **54**, 12004-12008.
7. Y. R. Zheng, M. R. Gao, Q. Gao, H. H. Li, J. Xu, Z. Y. Wu and S. H. Yu, *Small*, 2015, **11**, 182-188.
8. Y. Liu, H. Cheng, M. Lyu, S. Fan, Q. Liu, W. Zhang, Y. Zhi, C. Wang, C. Xiao, S. Wei, B. Ye and Y. Xie, *J. Am. Chem. Soc.*, 2014, **136**, 15670-15675.
9. S. Li, S. Peng, L. Huang, X. Cui, A. M. Al-Enizi and G. Zheng, *ACS Appl. Mater. Interfaces*, 2016, **8**, 20534-20539.
10. X. Zhao, H. Zhang, Y. Yan, J. Cao, X. Li, S. Zhou, Z. Peng and J. Zeng, *Angew. Chem. Int. Ed.*, 2017, **56**, 328-332.
11. S. Zhao, R. Jin, H. Abroshan, C. Zeng, H. Zhang, S. D. House, E. Gottlieb, H. J. Kim, J. C. Yang and R. Jin, *J. Am. Chem. Soc.*, 2017, **139**, 1077-1080.
12. Q. Dong, Q. Wang, Z. Dai, H. Qiu and X. Dong, *ACS Appl. Mater. Interfaces*, 2016, **8**, 26902-26907.
13. D. V. Shinde, L. D. Trizio, Z. Dang, M. Prato, R. Gaspari and L. Manna, *Chem. Mater.*, 2017, **29**, 7032-7041.